

Distribution of Fluorine in Hydroxyapatite studied by Infrared Spectroscopy

By Friedemann Freund* and Rolf M. Knobel, Mineralogisches Institut der Universität, Zülpicher Str. 49, D-5000 Köln-1, West Germany

In pure hydroxyapatite the O-H stretching and librational modes give rise to i.r. bands at 3 573 and 631 cm^{-1} . On introduction of F, the band at 631 cm^{-1} shifts to higher wavenumbers, ultimately to 641 and 647 cm^{-1} , and decreases in intensity. This shift can be correlated with the number n of OH groups in the chain sections between F which have the generalised form $\cdots \text{F HO (HO)}_n \text{HO:OH (OH)}_n \text{OH F} \cdots$. The 'tail-to-tail' configuration, $\cdots \text{HO:OH} \cdots$, gives rise to bands at 680 (bending) and 3 643 cm^{-1} (stretching). The OH bonded to one F gives rise to bands at 720 and 3 546 cm^{-1} . If OH is dispersed in a chain composed mainly of F, the configuration $\cdots \text{F OH F} \cdots$, the O-H stretching and bending bands lie at 3 540 and 747 cm^{-1} respectively.

HYDROXYAPATITE, $\text{Ca}_5(\text{OH})(\text{PO}_4)_3$, is the main constituent of dental enamel and has received much attention in recent years. The incorporation of fluoride ions into the structure of hydroxyapatite is thought to help prevent caries.¹⁻³ The degree of fluorination has been studied by many different methods, although surprisingly not by i.r. spectroscopy. Only the end members, hydroxy- and fluoro-apatite, have been studied extensively by both i.r. and Raman spectroscopy.^{4,5} Their vibrational spectra were unambiguously assigned by Fowler,⁵ using isotopic substitution. Fowler's results can be used to study and to assign the i.r. spectra of solid solutions between hydroxy- and fluoro-apatite.

EXPERIMENTAL

Eleven samples of apatite solid solutions were prepared by Schaecken *et al.*⁶ from $\text{Ca}[\text{HPO}_4]$, $\text{Ca}[\text{CO}_3]$, and CaF_2 reaction grade chemicals. The chemicals were thoroughly mixed as acetone slurries in an agate ball mill, then dried, pelletised, heated in open platinum crucibles to 1 000 °C, and held at this temperature for 3 h in a stream of nitrogen which had passed through 2 mol dm^{-3} $\text{Na}[\text{OH}]$ at 0 °C to remove CO_2 and to provide $p_{\text{H}_2\text{O}} = 4$ Torr.† The samples were cooled slowly, crushed, and again powdered in the ball mill. Three heating and homogenisation cycles were necessary in order to attain complete or nearly complete reaction. The fluorine content of the samples was determined using the methods of Ingram and May⁷ and Duff and Stuart.⁸ The samples were analysed by X-ray diffractometry. The results are given in the Table.

The samples were dried in air at 120 °C for several days. Three milligrams of each were then mixed with KI (750 mg; Uvasol, Merck) in an agate mortar and compressed in an evacuated 13-mm die at $ca. 5 \times 10^7 \text{ N m}^{-2}$. Potassium bromide pellets gave identical i.r. results. The i.r. spectra were recorded on a conventional Perkin-Elmer 225 and on a Digilab FTS-14 Fourier-transform spectrometer using 1 000 scans at a resolution of 1 cm^{-1} . A Globar heater was used as a source instead of the standard Nichrome coil.

† Throughout this paper: 1 Torr = (101 325/760) Pa.

¹ G. N. Jenkins, *Sci. Basis Med. Ann.*, 1971, 365.

² G. S. Ingram, *Caries Res.*, 1973, 7, 315.

³ O. Baker-Dirks, *Caries Res. Suppl.*, 1974, 8, 215.

⁴ D. M. Adams and I. R. Gardner, *J.C.S. Dalton*, 1974, 1505.

⁵ B. O. Fowler, *Inorg. Chem.*, 1974, 13, 194.

⁶ H. G. Schaecken, R. M. H. Verbeek, F. C. M. Driessens, and H. P. Thun, *Bull. Soc. chim. belges*, 1975, 84, 881.

⁷ B. L. Ingram and I. May, Geological Survey Research, U.S. Geol. Survey Prof. Paper 750-B, 180, 1971.

STRUCTURE OF APATITE

The structures of hydroxyapatite and of fluoroapatite have been determined by X-ray diffraction; that of hydroxyapatite has also been determined by neutron diffraction.^{9,10} The unit cell is hexagonal. The space group is $P 6_3$ for hydroxyapatite and $P 6_3/m$ for fluoroapatite. The structure contains linear chains of $[\text{OH}]^-$ or F^- ions parallel to the

Composition of $\text{Ca}_5\text{F}_x(\text{OH})_{1-x}(\text{PO}_4)_3$ solid solutions after Schaecken *et al.*⁶

x		Percentage of CaO present as second phase ^a
Found	Calc.	
b	0.00	1.0
b	0.03	0.9
b	0.06	0.9
0.097	0.10	0.7
0.191	0.20	0.7
0.31	0.30	0
0.38	0.40	0.6
0.51	0.50	0
0.66	0.65	0
0.76	0.80	0.4
0.95	1.00	0.3

^a As determined by X-ray analysis. ^b Not determined.

c axis.¹¹ The distribution of $[\text{OH}]^-$ and F^- along these chains in apatite solid solutions is the main topic of the present paper.

Figure 1 shows a side view of the linear chain with the ionic radii of the $[\text{OH}]^-$ and the F^- to scale. Neutron-diffraction studies¹⁰ have shown that the $[\text{OH}]^-$ is $ca. 0.3 \text{ \AA}$ off the plane of the three Ca^{2+} . If an F^- is included in the chain, ¹⁹F n.m.r. data show^{12,13} that both adjacent $[\text{OH}]^-$ ions orientate themselves in such a way that their protonic ends point towards the F^- . This gives one type of configuration $\cdots \text{OH F HO} \cdots$. The interatomic distances O-H \cdots O and O-H \cdots F as derived from the combined neutron diffraction and ¹⁹F n.m.r. results are also indicated

⁸ E. J. Duff and I. L. Stuart, *Analyt. Chim. Acta*, 1970, 52, 155.

⁹ A. S. Posner, A. Perloff, and A. F. Dioro, *Acta Cryst.*, 1958, 11, 308.

¹⁰ M. I. Kay, R. A. Young, and A. S. Posner, *Nature*, 1964, 204, 1050.

¹¹ D. McConnell, 'Apatite,' Springer, New York, 1973.

¹² R. A. Young, W. Van der Lugt, and J. C. Elliott, *Nature*, 1969, 223, 729.

¹³ W. Van der Lugt, D. I. M. Knotnerus, and R. A. Young, *Caries Res.*, 1970, 4, 89.

in Figure 1. In the undisturbed OH chain, schematically $\cdots \text{OH OH OH} \cdots$, the O-H distance within the $[\text{OH}]^-$ is 0.96 Å, while the distance $\text{H} \cdots \text{O}$ to the next $[\text{OH}]^-$ is 3.45 Å. The symmetrical $\text{H} \cdots \text{F}$ distances in the configuration $\cdots \text{OH F HO} \cdots$ are much smaller, 2.19 Å.¹³ This

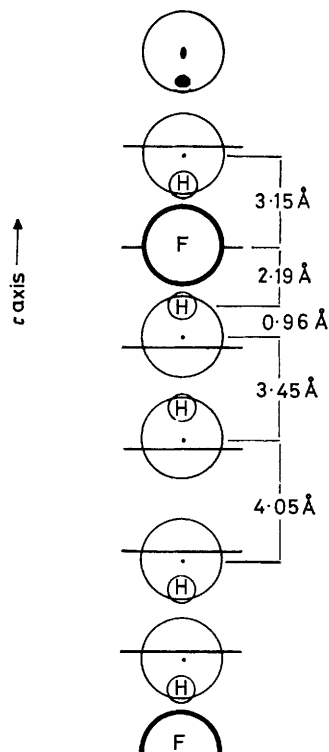


FIGURE 1 Side view of the (OH, F) chain in the apatite structure with the vertical 0.3 Å displacement of the $[\text{OH}]^-$ off the plane of the Ca^{2+} (indicated by the bar). In the uppermost $[\text{OH}]^-$ the anisotropic thermal motions of O^{2-} and H^+ at 300 K are shown (ref. 10)

$\text{H} \cdots \text{F}$ distance is very close to that expected if the F^- remains in the plane of the three Ca^{2+} and both $[\text{OH}]^-$, being 0.3 Å off the plane, orientate themselves as indicated. This particular OH F HO configuration should lead to another distinct O-H vibrational and OH librational mode of two $[\text{OH}]^-$ bonded to F.

If one considers a larger section of an $[\text{OH}]^-$ chain containing a few F^- , it becomes evident that somewhere between two F^- the dipole orientation of the $[\text{OH}]^-$ chain must reverse. This reversal will occur preferentially halfway between both F^- . This introduces a new configuration, $\cdots \text{HO:OH} \cdots$, which is expected to exhibit a different vibrational and librational spectrum. This configuration will be called 'tail-to-tail'. The 'head-on' configuration $\cdots \text{OH HO} \cdots$ is unlikely due to electrostatic repulsion.¹⁰ It would lead to a marked deviation from the OH dipole alignment parallel to the c axis which was excluded by single-crystal i.r. studies using polarised radiation.¹⁴

In summary, on the basis of structural data, the (OH, F) chain of apatite should contain at least three types of $[\text{OH}]^-$, possibly four, with distinguishable vibrational energies: (1) the 'normal' $[\text{OH}]^-$ in an extended $[\text{OH}]^-$ chain, schematically $\cdots \text{OH OH OH} \cdots$; (2) the 'tail-to-tail' configuration, $\cdots \text{HO:OH} \cdots$; and (3) the F-bonded $[\text{OH}]^-$ in the symmetrical configuration $\cdots \text{OH F HO} \cdots$. In F-rich chains containing only a few $[\text{OH}]^-$ one anticipates a fourth

distinguishable situation, (4), in which the F-bonded $[\text{OH}]^-$ is in an asymmetrical configuration, $\cdots \text{F F OH F F} \cdots$.

RESULTS

Figure 2 illustrates the changes occurring in the O-H stretching region at *ca.* 3600 cm^{-1} when increasing amounts of F^- are introduced into hydroxyapatite. The first set (a) of five spectra from hydroxyapatite containing 0, 3, 6, 10, and 19% F was normalised to the height of the component at 3573 cm^{-1} . The second set (b) of spectra from hydroxyapatite with 31, 51, 66, 76, and 95% F was normalised to the height of the component at 3540 cm^{-1} . As the OH content decreased (sample weight constant at 3.0 mg), the noise level increased noticeably for the last spectrum of nearly pure fluoroapatite containing only 5% OH).

While pure hydroxyapatite has only one O-H stretching band at 3573 cm^{-1} as predicted by the factor-group analysis,⁵ the introduction of F^- caused two new bands to appear at 3643 and 3544 cm^{-1} . Already at 31% F, the latter band,

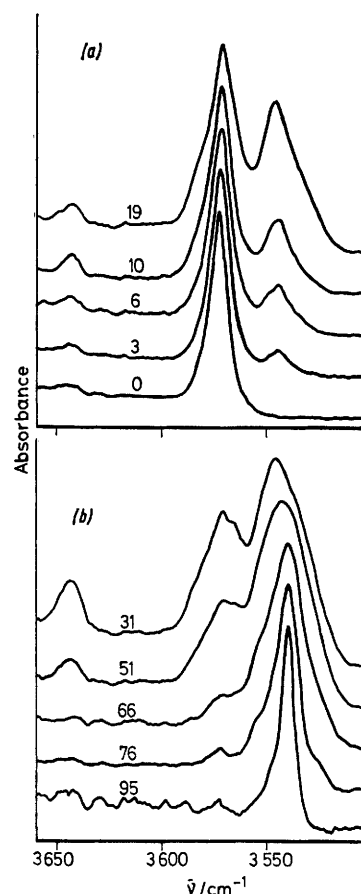


FIGURE 2 The OH stretching-band region of apatite solid solutions. For normalisation of (a) and (b) see text

now lying at 3546 cm^{-1} , had a larger relative intensity. It was a comparatively broad band and appears to be composed of at least two unresolved components. As the amount of F was further increased so that finally only a few $[\text{OH}]^-$ will be dispersed in a chain composed mainly of F^- , this band sharpened and shifted again to lower wavenumbers, 3540 cm^{-1} for 95% F. The behaviour of the

¹⁴ J. C. Elliott, *J. Dent. Res.*, 1962, **41**, 1251.

weak band to higher wavenumber at $3\ 643\text{ cm}^{-1}$ is peculiar. It was present only in the solid-solution spectra, going through an intensity maximum at *ca.* 31% F.

Figure 3 gives a compilation of the spectra in the 500–800 cm^{-1} region showing the complexity for the various apatite solid solutions. All the spectra in Figure 3 are on an identical intensity scale, so that the areas under the bands can be directly compared. The two strong bands at 601 and 571 cm^{-1} , which are purposely off scale, are due to the ν_4 mode of the PO_4 tetrahedra. They are quite obviously unaffected by the OH/F substitution along the chains. The valley

$\cdots\text{OH OH OH OH OH}\cdots$. The continuous displacement and intensity decrease of this band on introduction of F is shown in Figure 4, which is an enlargement of the 620–655 cm^{-1} region in Figure 4. In the range 0–19% F this band shifts continuously from 631 to 637 cm^{-1} without apparent change in shape or half-width ($\nu_{\frac{1}{2}} \approx 15\text{ cm}^{-1}$). The constant half-width shows that the F^- are more or less evenly distributed along the OH chains with no tendency to form clusters. For the sample containing 31% F this band seems to split into two maxima at

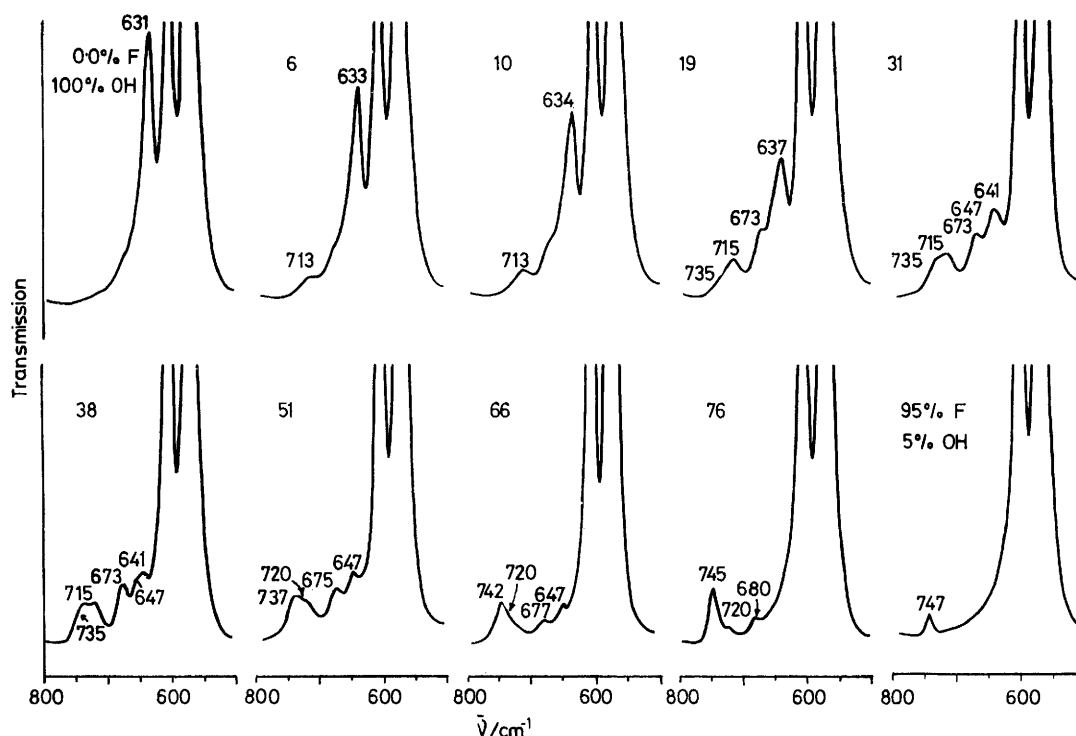


FIGURE 3 The OH librational-band region assigned to the $\text{Ca}_3\text{-OH}$ bending mode for apatite solid solutions

between the two bands may serve as a convenient internal intensity reference. The most prominent feature of Figure 3 is that the band at 631 cm^{-1} assigned to the $\text{Ca}_3\text{-OH}$ librational mode markedly shifts to higher wavenumbers and decreases in intensity as more F is introduced. Other weak bands appear, but only one survives in the 95% F spectrum, the weak band at 747 cm^{-1} . A detailed discussion of these spectra is given in the next section.

DISCUSSION

The $\text{Ca}_3\text{-OH}$ Librational Mode.—The spectra in Figure 3 show that the band at 631 cm^{-1} shifts, and new bands appear nearby, when F^- ions are introduced into the OH chain of hydroxyapatite. These bands are related to the three or four distinguishable type of $[\text{OH}]^-$ predicted above. First we discuss the behaviour of the band at 631 cm^{-1} .

This band in pure hydroxyapatite is due to the OH librational mode where the $[\text{OH}]^-$ forming the apex of the flat $\text{Ca}_3\text{-OH}$ trigonal pyramid executes a bending motion. The band is characteristic of the undisturbed OH chain,

641 and 647 cm^{-1} , of which only that at 647 cm^{-1} survives until 66% F.

The fact that the band at 631 cm^{-1} reacts so sensibly to the presence of F^- in the $[\text{OH}]^-$ chain indicates strong coupling between the OH dipoles along the OH chain. Three percent F means that, on average, about every 30th $[\text{OH}]^-$ is replaced by an F^- . This corresponds to a mean distance between fluorines of *ca.* 100 Å. The band at 631 cm^{-1} is undoubtedly due to the librational mode of the $[\text{OH}]^-$ surrounded by $[\text{OH}]^-$ in an infinitely long OH chain. As this chain decreases in length, the band at 631 cm^{-1} shifts. We can write down the shortest possible chain sections which still contain three, two, or one $[\text{OH}]^-$ ions in an OH surrounding: (a) $\cdots\text{HO:OH OH OH OH OH F}\cdots$; (b) $\cdots\text{HO:OH OH OH OH OH F}\cdots$; and (c) $\cdots\text{HO:OH OH OH F}\cdots$. The italicised $[\text{OH}]^-$ are the only ones in these chain sections which are neither bonded to an F (right) nor part of a 'tail-to-tail' configuration (left).

We assign the band at 647 cm^{-1} to the central $[\text{OH}]^-$

isolated $[\text{OH}]^-$ dispersed in a F chain, $\cdots \text{F F OH F F} \cdots$.

At low F contents (0–19%) one new band grows at $3\ 643\ \text{cm}^{-1}$, shifted to higher wavenumbers. This indicates a stiffening of the O–H bond such as one might expect for the ‘tail-to-tail’ configuration, $\cdots \text{HO:OH} \cdots$. Indeed, this band at $3\ 643\ \text{cm}^{-1}$ first increases in intensity with increasing F content, then decreases again, and vanishes above 50% F as one would expect for the $\cdots \text{HO:OH} \cdots$ configuration. Yet, there is some discrepancy in comparison with the band at $680\ \text{cm}^{-1}$ which was also assigned to the ‘tail-to-tail’ configuration: the band at $680\ \text{cm}^{-1}$ remains as a shoulder up to 76% F.

The band at $3\ 540\ \text{cm}^{-1}$ is sharp and narrow only for the 95% F sample. Its half-width is *ca.* $9\ \text{cm}^{-1}$, but increases rapidly to $30\ \text{cm}^{-1}$ at 51 and 31% while at the same time the maximum shifts to $3\ 546\ \text{cm}^{-1}$. This indicates that the band at $3\ 540$ – $3\ 546\ \text{cm}^{-1}$ has at least two components, probably more. It appears to be safe to assign this band to $[\text{OH}]^-$ bonded directly to F^- in any of the OH F^- configurations shown in Figure 5. The band at $3\ 573\ \text{cm}^{-1}$ on the other hand, which shifts slightly to $3\ 571\ \text{cm}^{-1}$ with increasing F content, may be assigned to $[\text{OH}]^-$ ions which are not directly adjacent to either F^- , or to a ‘tail-to-tail’ configuration. This band is broadened from 10-cm^{-1} halfwidth at 0% F to $15\ \text{cm}^{-1}$ at 19% F. The band shape suggests some further components which, however, cannot be resolved.

In conclusion, the three most distinguishable configurations derived for the OH–F chain [(1) undisturbed OH,

(2) OH bonded to F, and (3) ‘tail-to-tail’] can also be found in the region of the O–H stretching vibration, however with less resolution than in the region of the $\text{Ca}_3\text{-OH}$ librational modes.

Conclusions.—Both the $\text{Ca}_3\text{-OH}$ librational and the O–H stretching band of hydroxyapatite at 631 and $3\ 573\ \text{cm}^{-1}$ respectively sensibly react to the introduction of F^- into the linear OH chains. In particular, the band at $631\ \text{cm}^{-1}$ shifts markedly to higher wavenumber, ultimately to $647\ \text{cm}^{-1}$, and decreases in intensity. In addition, new bands appear nearby. Three, possibly four, bands or band components can be distinguished. They have been assigned to different configurations expected to be present in the chains containing $[\text{OH}]^-$ and F^- in various proportions. The four types are: (1) OH with OH neighbours only, $\cdots \text{OH OH OH} \cdots$; (2) OH in the ‘tail-to-tail’ configuration, $\cdots \text{HO:OH} \cdots$; (3) OH bonded to one F, $\cdots \text{OH OH F} \cdots$; and (4) OH surrounded by F only, $\cdots \text{F OH F} \cdots$. The shifts observed mainly for the band at $631\ \text{cm}^{-1}$ can be correlated with the average number of OH of the same configuration in the chain section between F ions, generally $\cdots \text{F HO (HO)}_n \text{HO:OH (OH)}_n \text{OH F} \cdots$. The partly resolved bands at 647 and $641\ \text{cm}^{-1}$ have been assigned to chain sections with $n = 1$ and 2 respectively.

We thank Dr. R. M. H. Verbeek of the Rijksuniversiteit in Ghent, Belgium, who kindly provided the samples, and the Bayer AG, Leverkusen, in particular to Dr. G. Bayer and H. Devrient who ran the i.r. spectra.

[6/2151 Received, 22nd November, 1976]